Magazine of Civil Engineering

ISSN 2712-8172

journal homepage: http://engstroy.spbstu.ru/

DOI: 10.34910/MCE.107.14

# Isotropic damage model to simulate failure in reinforced concrete beam

***W.A. Al-Kutti****[a]*, T.C. Chernykh***[b]**

[a] *Imam Abdulrahman bin Faisal University, Dammam, Saudi Arabia*

[b] *South Ural State University, Chelyabinsk, Russia*

**E-mail: wasalem@iau.edu.sa*

**Keywords:** concrete model, isotropic damage, flexural loading, finite element analysis

**Abstract.** This study investigates the possibility of simulating the behavior of reinforced concrete (RC) beams subjected to flexure using a simplified elasto-isotropic damage. The phenomenological damage concept was used to evaluate stress-induced damage. The influence of the damage on elastic stiffness was used to evaluate mechanical performance with respect to material degradation. RC beams damaged in flexure with 40 %, 60 %, 75 %, and 90 % of ultimate flexural loading were modeled using the COMSOL Multi-physics finite element package to simulate mechanical performance of RC concrete beams. The proposed elasto-damage model predicted the ultimate load of the RC beams with 1 % estimated error. The proposed model showed similar ability to predict the axial strain for the reinforcement steel as the maximum strain in tensile reinforcement. The accuracy of these results were compared with other constitutive models for concrete such as elasto-plastic damage model reported in literature. The outcome of this research paper provides engineers with a simplified approach for analyzing the behavior of RC beams subjected to flexural loading using elasto-damage model.

## *1. Introduction*

Damage mechanics refer to constitutive models characterized by diminished stiffness or a reduction of the secant modulus. Kachanov [1] introduced the concept for use in creep-related models and then later adapted it to describe the progressive failure of metals and composites and to model the behavior of the materials under fatigue. Damage models are used to describe the strain-softening behavior of concrete.

Researchers have developed damage models of varying degrees of sophistication to model damage on material such as concrete [2–21]. Two main approaches have been proposed in how the stiffness degradation to be modeled. Some researchers [3–14] have used elastic and plastic analysis coupled with damage variables representing the reduction in the stiffness. Others [15–20] coupled damage with the elastic analysis.

Besides, several mechanical loading on concrete have been modeled using elastic and plastic analysis coupled with damage. Sun et al. [4] studied the damage evolution and the plasticity development in concrete materials subjected to freeze-thaw and proposed a cohesion reduction parameter to improve the accuracy of previous damage constitutive models for concrete materials. Similar approach was used by Sarikaya and Erkmen [5] in which plastic-damage model for concrete under compression was modeled. Javanmardi and Maheri [6] developed a new algorithm for predicting crack initiation and growth direction in 3D solid concrete using anisotropic damage-plasticity model. In the study, three benchmark problems solved using the proposed algorithm were compared with experimental data and those of other numerical simulations. Javanmardi and Maheri [6] concluded that the proposed anisotropic damage-plasticity model predicted well the crack development and the numerical results match well with the experimental results previously reported in the literature.

Al-Kutti, W.A., Chernykh, T.C. An isotropic damage model to simulate failure in reinforced concrete beam. Magazine of Civil Engineering. 2021. 107(7). Article No. 10714. DOI: 10.34910/MCE.107.14

In a comprehensive study, Benin et al. [7] proposed a methodology for identification of mechanical characteristics of the nonlinear material model for concrete. Benin et al. [7] investigated the damage accumulation under monotonous and cyclic loading. The material parameter identification procedure of elastic-plastic-damage concrete model was proposed and validated. In recent study, Bilal et al. [8] proposed a new plastic damage model for concrete with a novel stress decomposition to account for shear induced damage. In their model, a thermodynamic approach was used to derive the constitutive model.

For the elasto-damage model, Labadi and Hannachi [15] proposed a new damage criterion defined as an equivalent strain norm and reported that simple isotropic damage model coupled with the nonlinear elastic deformation can predict accurately the mechanical behavior of concrete. Similar study was conducted by Tao and Phillips [16] where they presented a concrete model based on the elasto-damage model for concrete subjected to bi-axial loading. The numerical and matched well with the experimental results.

Although the above researchers concluded on the suitability of using the elastic and plastic analysis coupled with damage in concrete compared with the elasto-damage model, several others [15–20] debate that the elaso-damage model can predict well the behavior of concrete with less complexity and minimum convergence problem associated in the elasto-plastic damage models. The primary objective of this study is to explore the possibility to simulate the failure of RC beams in flexural using isotropic damage parameters based on an elastic-damage constitutive model. To achieve objective, finite element analysis was conducted using COMSOL FE package and an experimental program was developed to verify the numerical results. The outcome of this research paper will provide more experimental and numerical studies on the suitability of using elasto-damage model on simulation the failure of RC beams subjected to flexural loading.

Amongst the numerous studies modeling damage Mazars et al. [2] first evaluated the influence of damage on the material responsiveness of concrete and evaluated how degradation affected the elastic stiffness of the material. This was then used to model a scalar damage parameter (*d)*. Their research quantified this relationship as:

$$\sigma = E\varepsilon \tag{1}$$

$$E = (1-d)E_o \tag{2}$$

where $E_o$ and $E$ are the secant (undamaged) and (damaged) modulus, and $d$ is a scalar damage variable. Taher et al. [3] developed an elasto-damage model for concrete using a constitutive law proposed by Popovics [22] for stress-total strain relationship of plain concrete subjected to uniaxial tensile and compressive stress in the form of:

$$\frac{\sigma}{\sigma_u} = \frac{m\left(\frac{\varepsilon}{\varepsilon_u}\right)}{m-1+\left(\frac{\varepsilon}{\varepsilon_u}\right)^m} \tag{3}$$

where $\sigma_u$ and $\varepsilon_u$ are peak stress and strain, respectively, and $m$ is a parameter dependent on $\sigma_u$. Using equation [3], a relationship between the moduli and damage variable could be obtained as shown in Fig. 1 as the following:

$$E = \frac{\sigma}{\varepsilon} = \frac{m\frac{\sigma_u}{\varepsilon_u}}{m-1+\left(\frac{\varepsilon}{\varepsilon_u}\right)m} \tag{4}$$

$$E_o = E(\varepsilon = 0) = \frac{m\sigma_u}{(m-1)\varepsilon_u} \tag{5}$$

The scalar damage becomes:

$$d_c = 1 - \frac{E}{E_c} = 1 - \frac{m_c - 1}{m_c - 1 + \left(\frac{\varepsilon_x}{\varepsilon_u}\right)^{m_c}} \; for \varepsilon_x < 0 \; (Compression) \quad (6)$$

$$d_t = 1 - \frac{E}{E_t} = 1 - \frac{m_t - 1}{m_t - 1 + \left(\frac{\varepsilon_x}{\varepsilon_u}\right)^{m_t}} \; for \varepsilon_x < 0 \; (Tension) \quad (7)$$

Where, $E_c$ and $E_t$ are the undamaged secant moduli representing compressive and tensile in units of MPa, respectively. $m_c$ and $m_t$ are the material parameters for compression and tensile induced damage respectively, and $\varepsilon_x$ is the total strain in mm/mm.

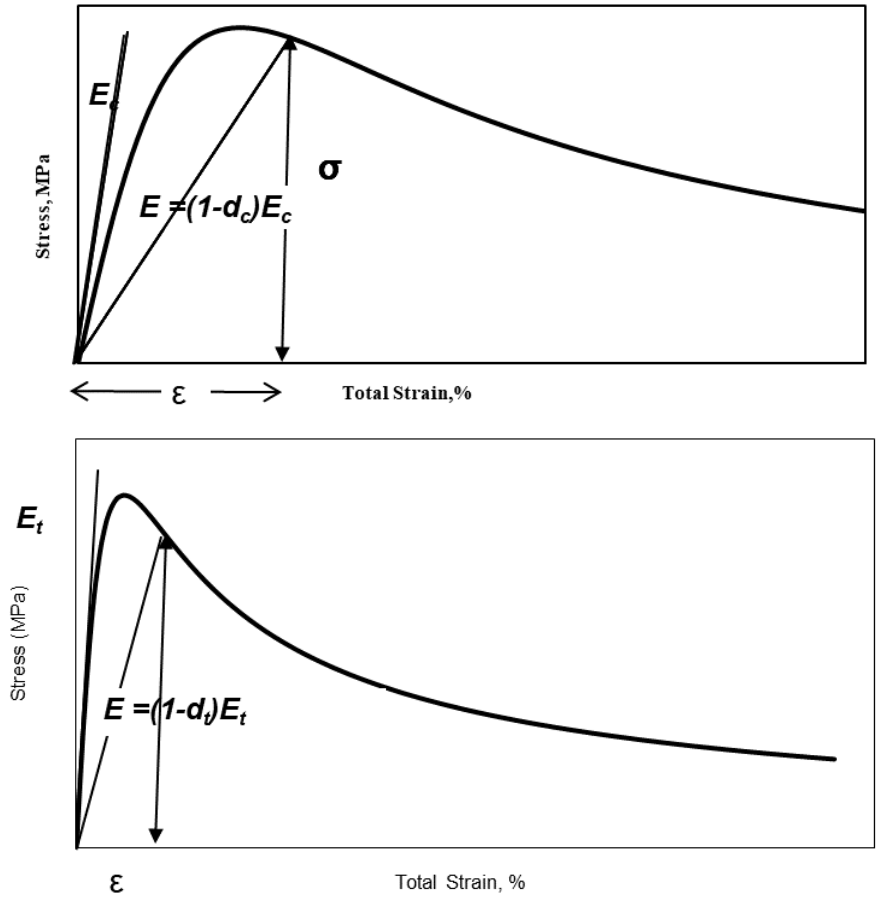


**Figure 1. The relationship between scalar damage and uniaxial tensile/compressive stress-total strain curve.**

# 2. Methods

## 2.1. Testing plan

To achieve the objectives of this study, different concrete samples including reinforced concrete (RC) beams and concrete cylinders were used. Four levels of mechanical loading were applied on the concrete samples as a percentage of the compressive strength of the concrete after 28 days of curing. Using the experimental results, numerical simulation of the mechanical loading leading to damage, would be achieved.

## 2.2. Cement, aggregates and mix design

ASTM C 150 Type I Portland cement was utilized in all the concrete mixes. Limestone coarse aggregate was used along with dune sand as fine aggregates. The specific gravity and absorption of the coarse and fine aggregates are shown in Table 1. The fine and coarse aggregates were combined such that the coarse aggregate constituted 62 % of total aggregates. The grading of coarse aggregates was

selected conforming to ASTM C 33 and is shown in Table 2. Potable water was used for casting and curing all the concrete specimens and the water to cement ratio was 0.40. Details of the mix ingredients are shown in Table 3.

***Table 1. Absorption and Specific Gravity of the Coarse and Fine Aggregates.***

| Aggregate | Absorption (%) | Bulk Specific Gravity |
|---|---|---|
| Coarse AggregateCoarse Aggregate | 2.5 | 2.54 |
| Fine aggregate | 0.5 | 2.64 |

***Table 2. Grading of Coarse Aggregates.***

| SIZE (in) | % Retained | Cumulative (% Retained) | Cumulative (% Passing) |
|---|---|---|---|
| ¾ | 0 | 0 | 100 |
| ½ | 35 | 35 | 65 |
| 3/8 | 35 | 70 | 30 |
| 3/16 | 20 | 90 | 10 |
| 3/32 | 10 | 100 | 0 |

***Table 3. Mixes Ingredients.***

| Concrete Type | Cement Content (kg/m$^3$) | w/c | Admixture (kg/m$^3$) | Aggregate (kg/m$^3$) |
|---|---|---|---|---|
| OPC | 480 | 0.40 | 3.25 (Conplast SP-440) | 1725 |

## *2.3. Specimens*

In this study, the experimental program consists of the following parameters: Ordinary Portland Concrete (**OPC**) and five levels of mechanical loading leading to damage applied on the concrete beams and cylinders as a percentage of compressive strength of concrete after 28 days of curing. The following concrete specimens were cast from each concrete mix:

(i) 10 reinforced concrete (RC) beams (150 × 150 × 1200 mm) for determining the effect of mechanical damage. Fig. 2 shows the cross-section details of the RC beams. Strain gauges were placed to monitor the mechanical behavior of the RC beams when subjected to the four-point flexural test as shown in Fig. 3.

(ii) 6 cylindrical concrete specimens (76 × 150 mm) for the determination of compressive strength.

## *2.4. Curing*

After casting, the RC concrete beams were covered with a wet towel for 24 hours and cured in the laboratory under dry conditions for one month. The cylindrical concrete specimens were demolded and cured in water tanks for 28 days.

## *2.5. Laboratory Tests*

The following tests assessed the mechanical properties in damaged and undamaged concrete:

### *2.5.1 Compressive strength*

Concrete specimens were tested for compressive strength after 28 days of water curing. The specimens were capped with a sulfur compound. Prior to capping, the diameter and height of the specimens were measured. The capped specimens were then placed in a compression testing machine (3000 kN capacity). The compressive strength was determined according to ASTM C 39.

### *2.5.2 Flexural Test*

After the beams cured for 28 days under dry laboratory conditions, two RC beams as shown in Figure 4 were loaded by a four point's flexural loading test to failure to determine the ultimate bending moment capacity. During loading, the strain in the reinforcement bars at the bottom of the RC beams was monitored as well as the strain in concrete in the compressive zone. Besides, the deflection at the mid span of the beams was measured using linear variable differential transformers (LVDT). To create mechanical induced

damage, eight RC beams were loaded at 40 %, 60 %, 75 % and 90 % of the ultimate loading capacity of the beams.

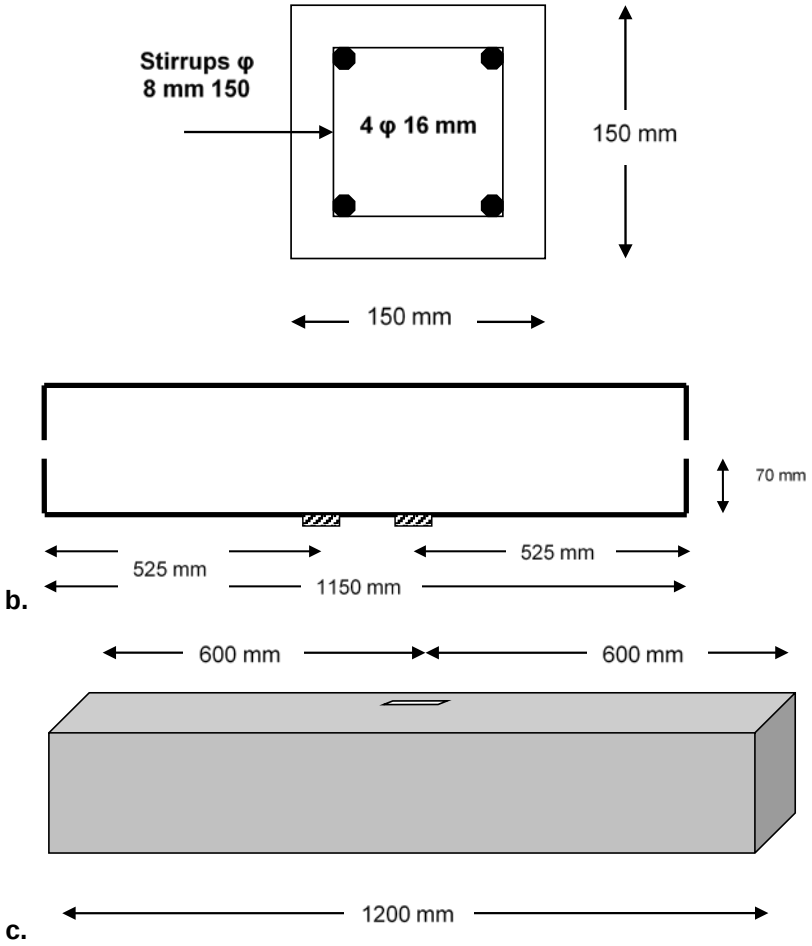


**Figure 2. (a) RC beam cross section details, (b) Arrangement for strain gauges in reinforcement bars, (c) Arrangement of strain gauge in concrete.**

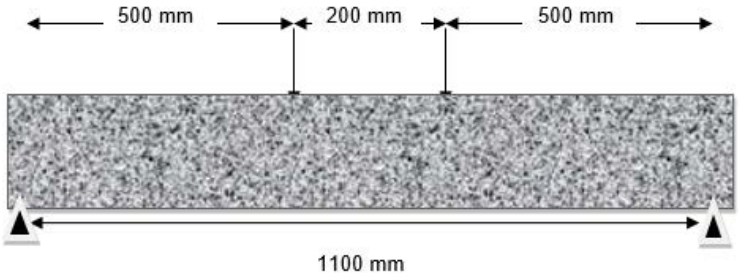


**Figure 3. Four-point flexural loading.**

**Figure 4. Measurements of the strains in reinforcing bars and the deflection at mid span using data logger.**

# 3. Results and Discussion:

## 3.1. Mechanical Behavior

The results of for the mid span deflection, strain in the reinforcement at mid span all, cracking load and maximum load are mentioned in Table 4 and Fig. 5 through 10. From Fig. 5 through 10, it can be observed that the elastic zone ended at the first cracking loads which were varied between 6.5 to 8 kN with an average of 7.5 kN for all levels of loading. Besides. These results match well with the cracking load calculated using the ACI approach [23] where it was found to be about 7 kN. However, the ACI approach shows higher stiffened behavior than the experimental results after the cracking load.

***Table 4. Details of Cracking and Maximum Flexural Loading, Mid Span deflection and Strains in Reinforcement for Damaged RC Beams.***

| RC Beams | First Crack Load, $P_{cr}$ (kN) | Maximum Load, P (kN) | Mid Span Deflection (mm) | Strain in Reinforcement Steel at Mid Span (μm) |
|---|---|---|---|---|
| B40 | 7.5 | 38 | 2.5 | 1500 |
| B60 | 6.5 | 62 | 4.5 | 2350 |
| B75 | 7.5 | 75 | 5.5 | 2600 |
| B90 | 7.5 | 84 | 7.0 | 3400 |
| B100 | 8 | 98 | 9.0 | 3750 |

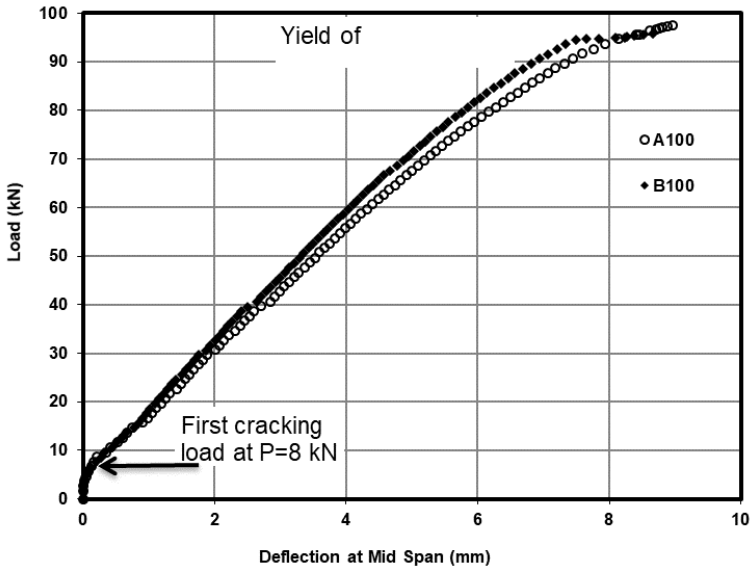


**Figure 5. Load – mid span deflection curve for A100 and B100 beams.**

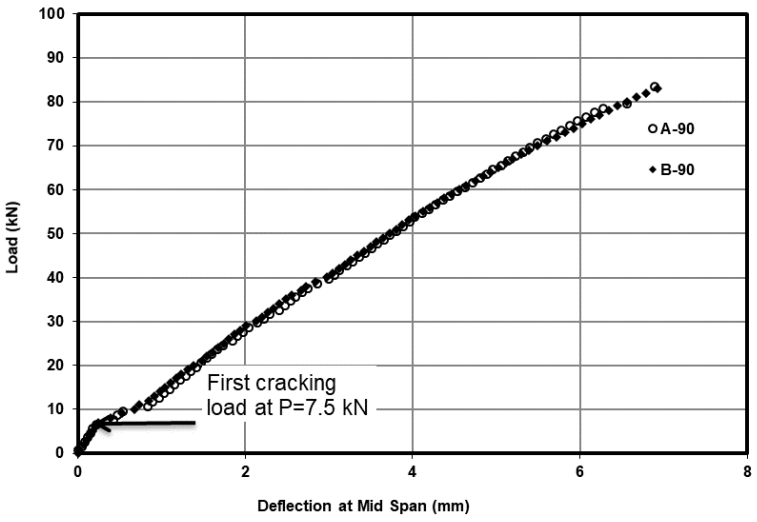


**Figure 6. Load – mid span deflection curve for A90 and B90 beams.**

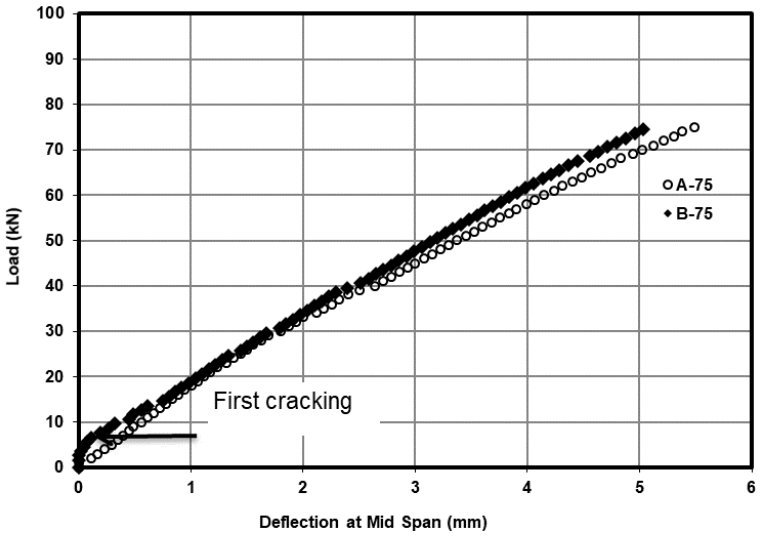


**Figure 7. Load – mid span deflection curve for A75 and B75 beams.**

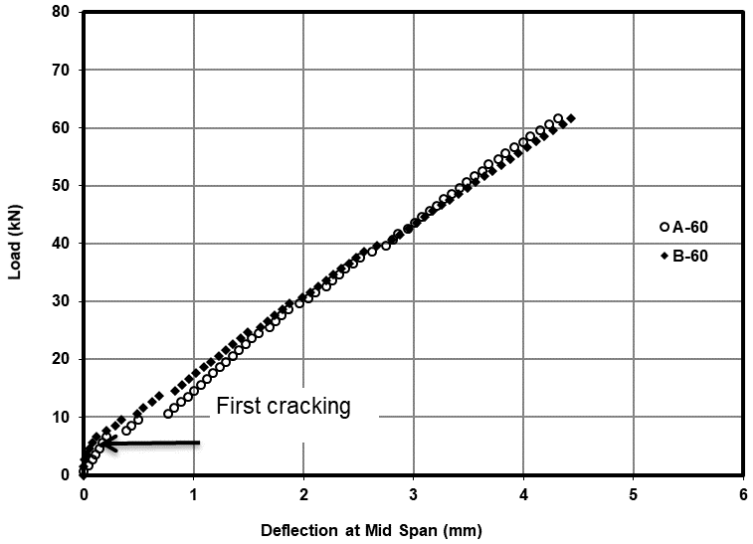


**Figure 8. Load – mid span deflection curve for A60 and B60 beams.**

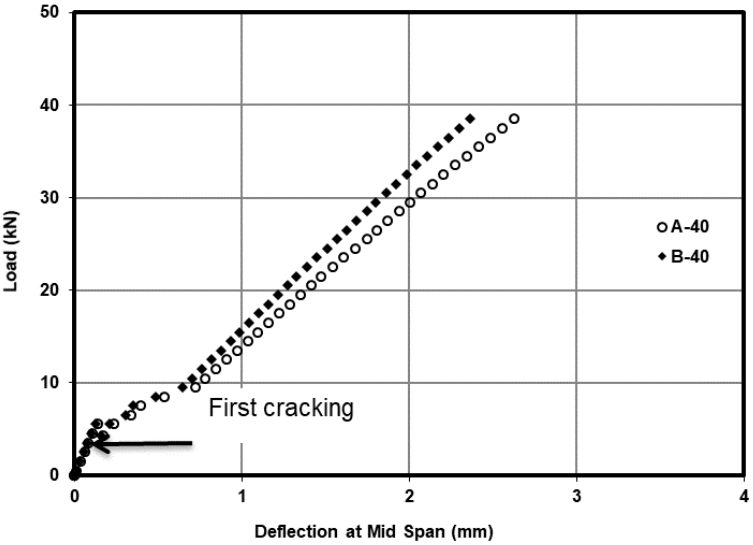


**Figure 9. Load – mid span deflection curve for A40 and B40 beams.**

The experimental results of the reinforcement axial strain vs. mid span deflection up to failure loading is presented in Fig. 11. The axial strain measurements were monitored at the maximum moment zone about 500 mm from the support and was found to be about 3500 μm at the maximum mid-span deflection of about 9 mm. which indicating the yielding of the reinforcement steel. The cracking map of the RC Beams

at the failure loading is presented in Fig. 12. The maximum cracking depth was found to be about 90 mm. The calculated value of $z$ , based on ACI approach [23], was found to be about 92.4 mm from bottom of the beam which indicates a very close results between the experimental and the ACI approach [23].

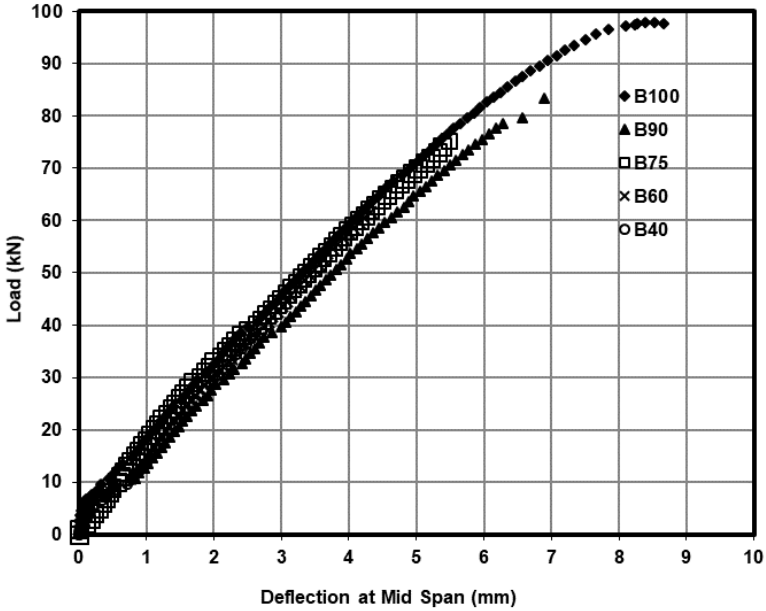


**Figure 10. Load – mid span deflection curve for 40 %, 60 %, 75 %, 90 % and 100 % loading.**

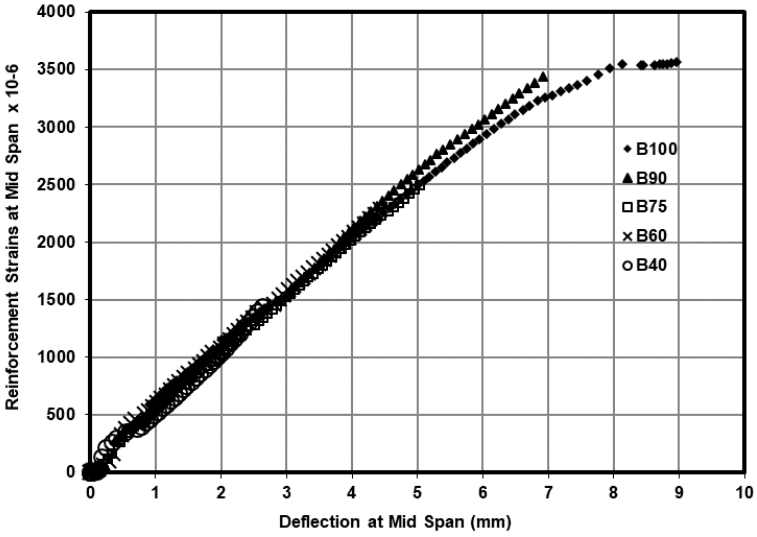


**Figure 11. Strain in reinforcement vs mid span deflection curve for 40%, 60%, 75%, 90% and 100% loading.**

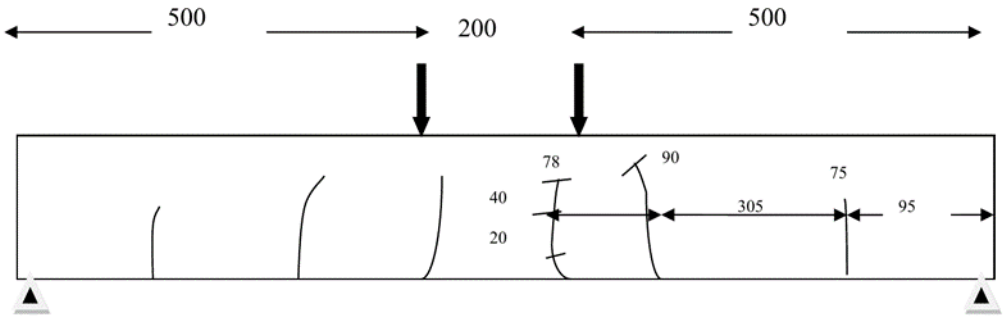


**Figure 12. Cracking map of up to 100% loading.**

### 3.2. COMSOL Simulation Steps

COMSOL finite element software [24] was used to simulate flexural behavior of RC using Scalar Damage Parameter as described in equations [1] to [7]. The Drucker-Prager yield criterion was first used to simulate the mechanical behavior of the RC beams in which the Drucker-Prager yield criterion was formulated as

$$f\left(I,\sqrt{J}\right)=\sqrt{J}+\alpha I=k \tag{8}$$

Where, $I=\sigma_{kk}$ is the hydrostatic component of the stress tensor, $J=\frac{1}{2}S_{ij}S_{ji}$ is the deviatoric stress tensor invariant, $\alpha$ and $k$ are materials constants which can be related to the friction angle ($\varphi$) and cohesion ($c$) of the Mohr-Coulomb criterion. For plane stress, the relation between the parameters are as follows:

$$\alpha=\frac{\sin\varphi}{\sqrt{3}} \qquad k=\frac{2}{\sqrt{3}}c\cos\varphi \tag{9}$$

By the calibration of the experimental P-Δ curve as shown in Fig. 6 through 10, the cohesion $c$ and the friction angle $\varphi$ were estimated by parametric study and using COMSOL model. Fig. 13 shows the finite element for the RC beams including boundary conditions of the RC beams. The steel reinforcement was modeled as a plate representing the area of reinforcement in the beam with the same thickness of the concrete section. Von Mises material model was used for the steel reinforcement in which $E_s$ and $F_{ys}$ was 19000 MPa and 560 MPa, respectively. A flow chart for steps required is presented in Fig. 14. Tables 5 shows the parameters used in the COMSOL model.

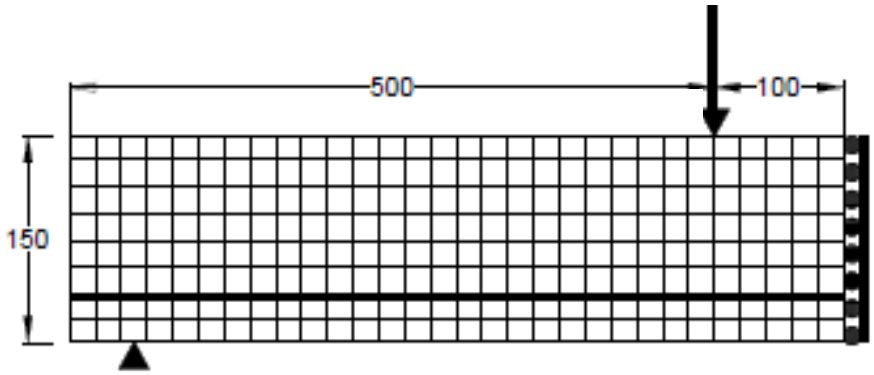


**Figure 13. Finite Element Modeling of the RC Beams Subjected to Flexural Loading.**

***Table 5. COMSOL model parameters.***

| COMSOL Commands | COMSOL Expression/Parameters | Value |
|---|---|---|
| Constants | $m_t$ | **1.46** |
| | $m_c$ | **3.45** |
| | $c$ | 4.8 MPa |
| | $\varphi$ | 53o |
| | $f_{cr}$ | 4 MPa |
| | $f_u$ | 50 Mpa |
| | $\varepsilon_{cr}$ | 1.55e-4 |
| | $\varepsilon_u$ | 2.3e-3 |
| | $F_{ys}$ | 560 Mpa |
| | $\alpha$ | 2.39 |
| | $\beta$ | 15.6 |

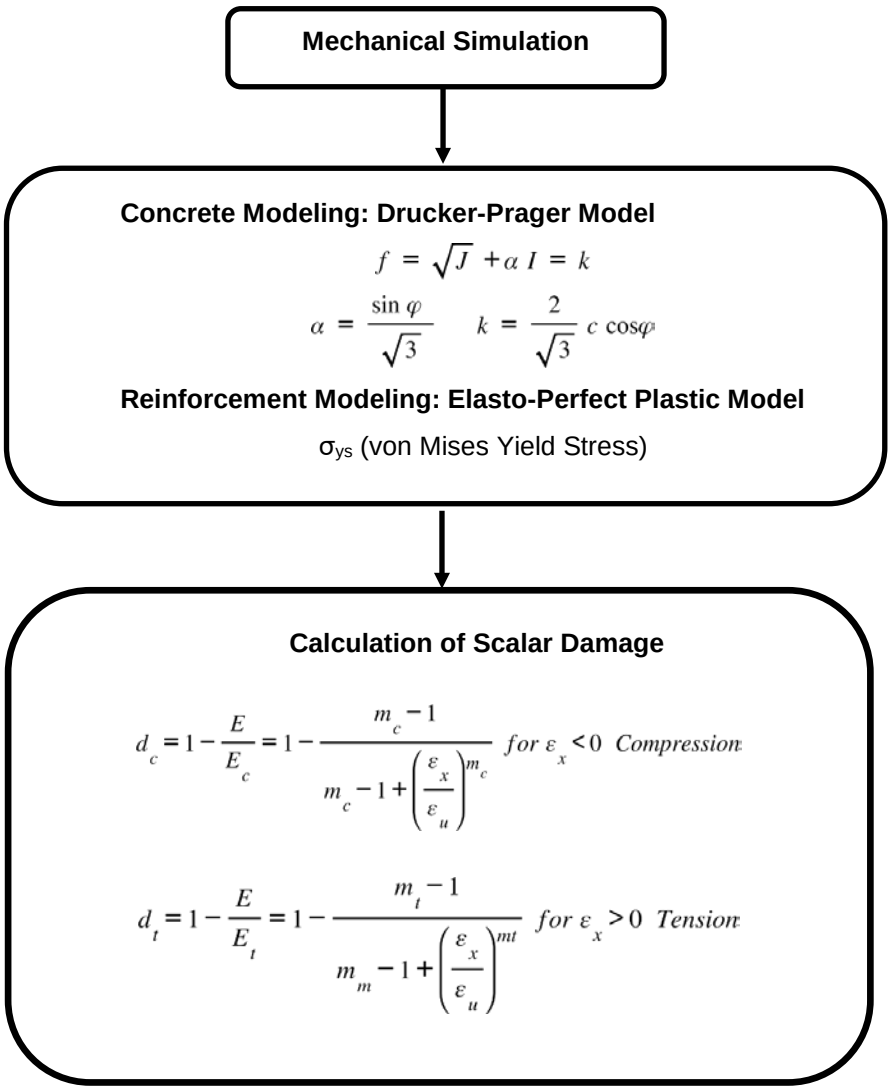


**Figure 14. Flow chart for the simulation of mechanical damage in RC beams.**

## *3.3. COMSOL Simulation of Mechanical Behavior*

### *3.3.1 Load-deflection curves and Reinforcement Axial Strain*

A comparison between the numerical simulation and ACI [23]/experimental results for load-deflection curve is shown in Fig. 15. COMSOL solution has predicted a cracking load at about 7.25 kN which match well the ACI [23] and the average experimental cracking load which were found to be about 7 and 7.5 kN, respectively. This result indicated that the proposed numerical model can predict the cracking load with about 3.5 % error. As the model is assuming full bond between the reinforcement and the concrete, it can be noticed from Fig. 15 that the COMSOL solution tends to provide more stiffened behavior similar to ACI calculation [23]. However, the COMOSL predicted an ultimate load with 94 kN compared to 95 kN achieved in the experimental flexural tests with 1 % error. The COMSOL model showed similar ability to predict the axial strain for the reinforcement steel and from Fig. 16, it can be noticed that the COMSOL maximum strain in tensile reinforcement was found to be 3500 μm at the maximum mid-span deflection of about 7.5 mm these results match well with the experimental results. The accuracy of these results were compared with other constitutive models for concrete such as the concrete damage-plasticity (CDP) model which have been recently investigated by Abdulsamee et al. [25]. Using CDP model ABAQUS package, Abdulsamee et al. [25] have reported an 4 % and 1 % error in estimating the crack and ultimate loads in RC beams, respectively. These results match well with elastic- damage model used in this study. Others such as Mohammed et al. [26] reported up to 7 % error in predicting the ultimate load when using models based on the classical orthotropic smeared crack formulation and crack band model [26].

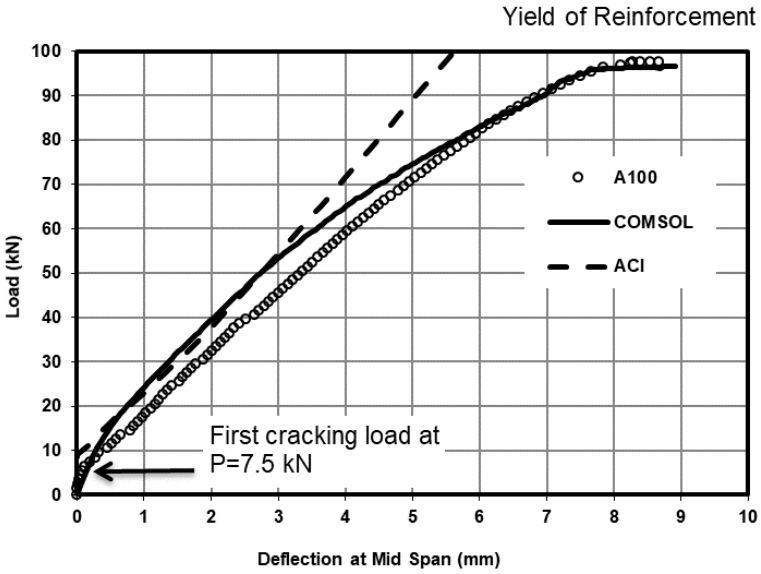


**Figure 15. Comparison between Numerical Simulation ACI/ Experimental Results for load- deflection curve.**

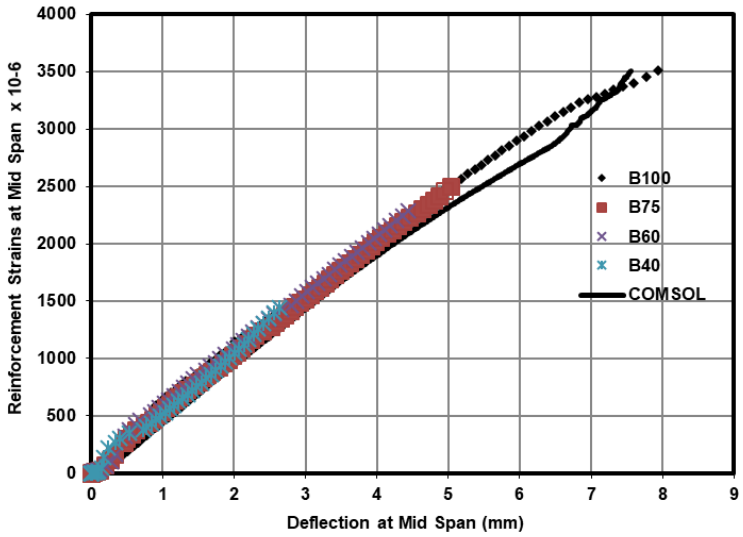


**Figure 16. Comparison between Numerical Simulation ACI/ Experimental Results for Reinforcement Axial Strain.**

### *3.3.2 Normal Stress $S_x$*

To verify the ability of the COMSOL model to simulate the mechanical behavior of the RC beams, two-dimensional stress and strain results were plotted. Fig. 17 demonstrates the normal stress distribution ($S_x$) along the RC beam subjected to 90 % of ultimate flexural loading. As expected, at this level of flexural loading which approached the failure load of the beam, the maximum compressive stress was about 50 MPa and the tensile stress in the reinforcement was about 560 MPa which means that the reinforcement reached its yielding state. More details could be observed in Fig. 18, where the normal stress distribution ($S_x$) along the cross section of the RC beam is presented, and it can be noted that the compressive zone is fixed at 60 mm from the top of the RC beam.

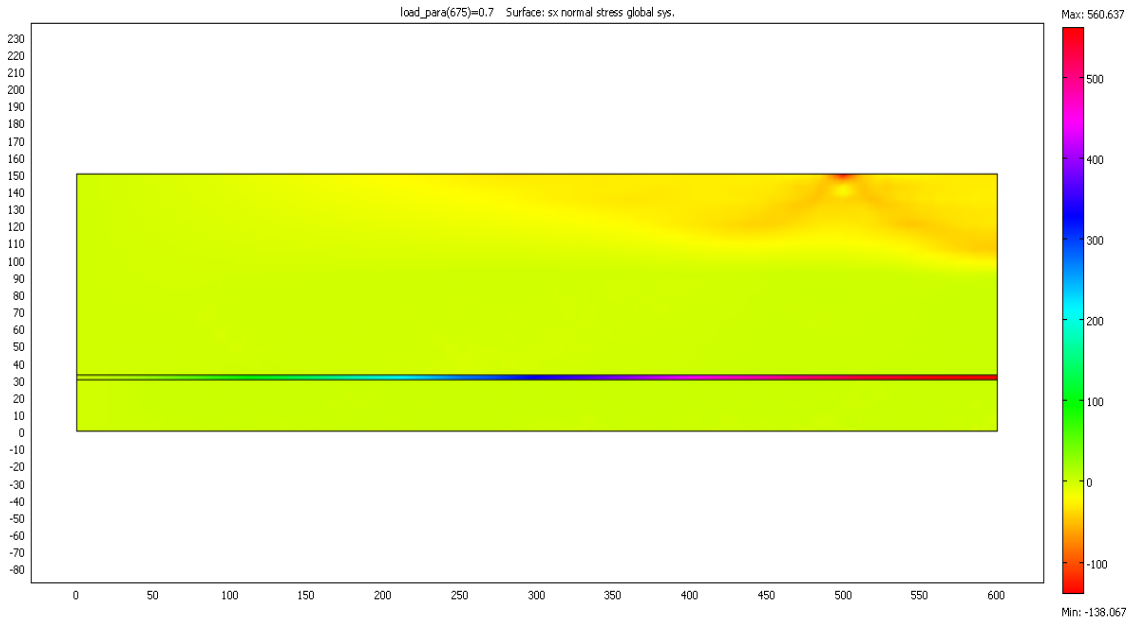


**Figure 17. Normal Stress ($S_x$) for B90.**

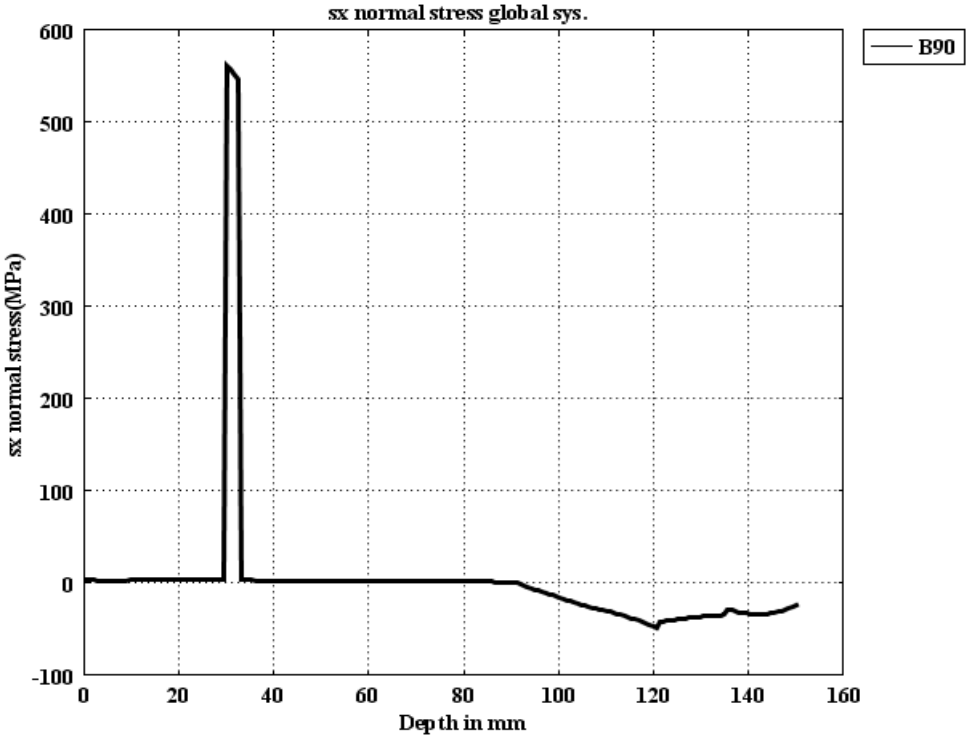


**Figure 18. Normal Stress ($S_x$) Distribution at Constant Moment Zone ($x$ = 550 mm from Support for B90).**

### *3.3.3 Normal Strain $\varepsilon_x$*

Two-dimensional simulation using the COMSOL model was conducted for normal strain ($\varepsilon_x$) and the results were plotted as in Fig. 19 & 20. When the RC beam loaded up to 90 % of its flexural loading, the normal strain in the compressive zone in the concrete approached a value of $3.5 \times 10^{-3}$ as shown in Fig. 19 and 20, which is very close to the ultimate concrete values suggested by ACI. The normal strain in the reinforcement increases as more flexural load applied on the RC beam and reached a value of $3 \times 10^{-3}$ which matches well with the experimental results for the normal strain in the reinforcement at 90 % of flexural loading which was about $3.5 \times 10^{-3}$ as shown in Fig. 11. The accuracy of the prediction for the strains using the scalar model was reported by Stéphanie et al. [27] where they concluded that the scalar damage model provides accurate prediction for the structural behavior in concrete elements when failure is mainly due to uniaxial extension.

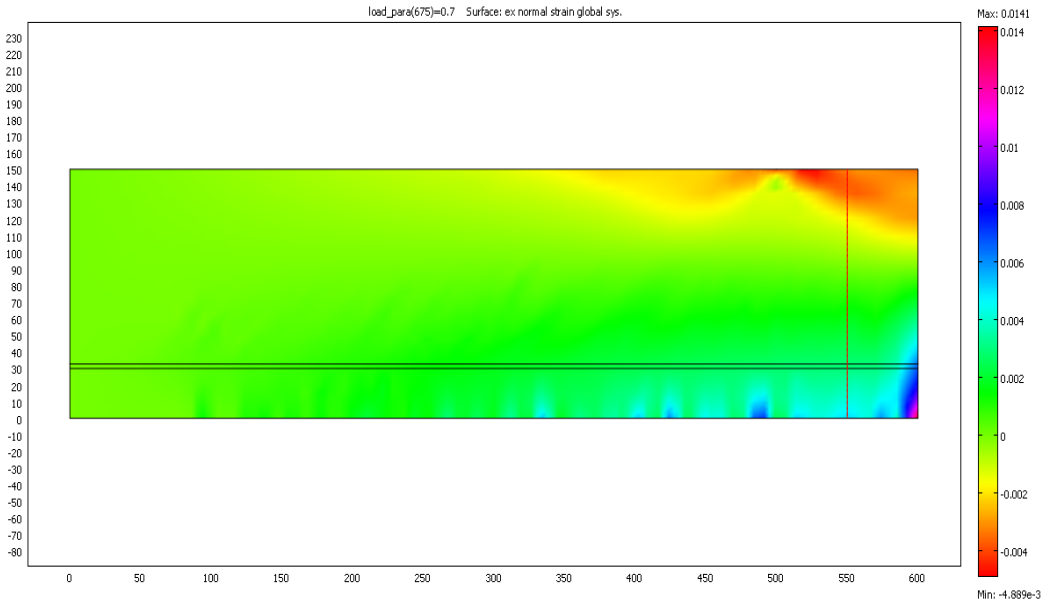


**Figure 19. Normal Strain $\varepsilon_x$ for B90.**

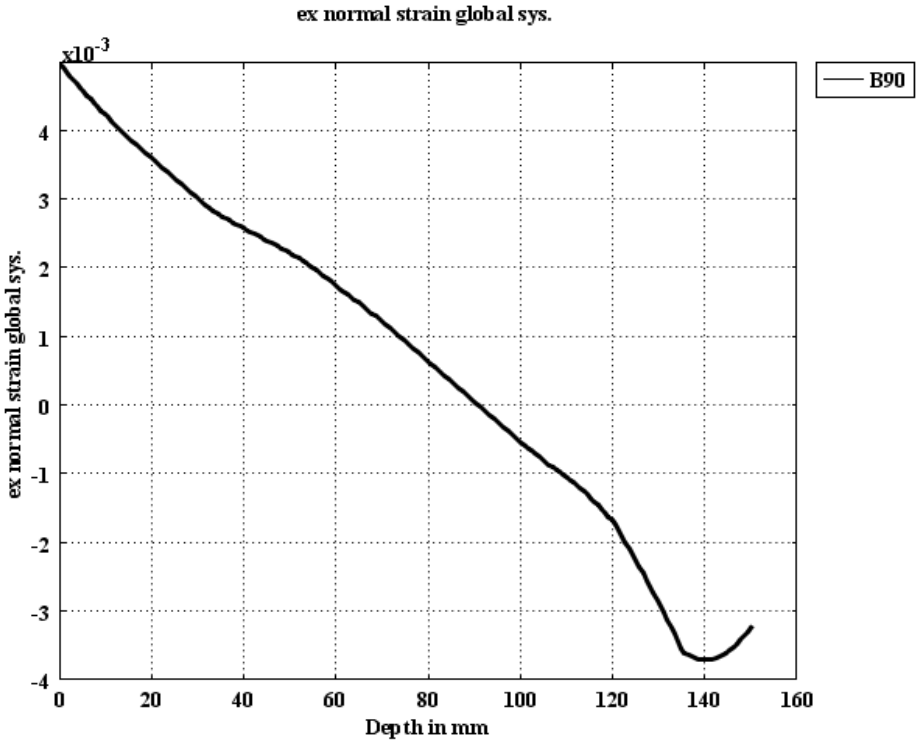


**Figure 20. Normal Strain $\varepsilon_x$ Distribution at Constant Moment Zone ($x$ = 550 mm from Support for B90).**

### *3.3.4 COMSOL Simulation of Mechanical Damage*

The two-dimensional damage distribution at 90% and failure loading for half of the reinforced concrete beam span (L/2 = 600 mm) are shown in Fig. 21 and 22. Fig. 21 shows the damage distribution in the RC beam subjected to 90 % of its ultimate flexural loading. From Fig. 21, it can be observed that a significant increase in compressive damage of about 0.90 was developed under point loading and these values decreased to 0.65 at the constant moment zone. When observing the tensile zone, it can be noted that there was more development in tensile damage especially towards the support because of the increase of the tensile stress with the increase of the applied flexural loading and the depth of the damage which increased up to 90 mm from the region between 150 mm from the support up to the mid span of the RC beam. At failure load, the compressive damage increased up to 0.90 with a depth of 50 mm while the damage in the tensile zone was up to 0.90 at a 90 mm depth from the bottom of the RC beam which indicates the development of a full crack in the RC beam at failure as shown in Fig. 22.

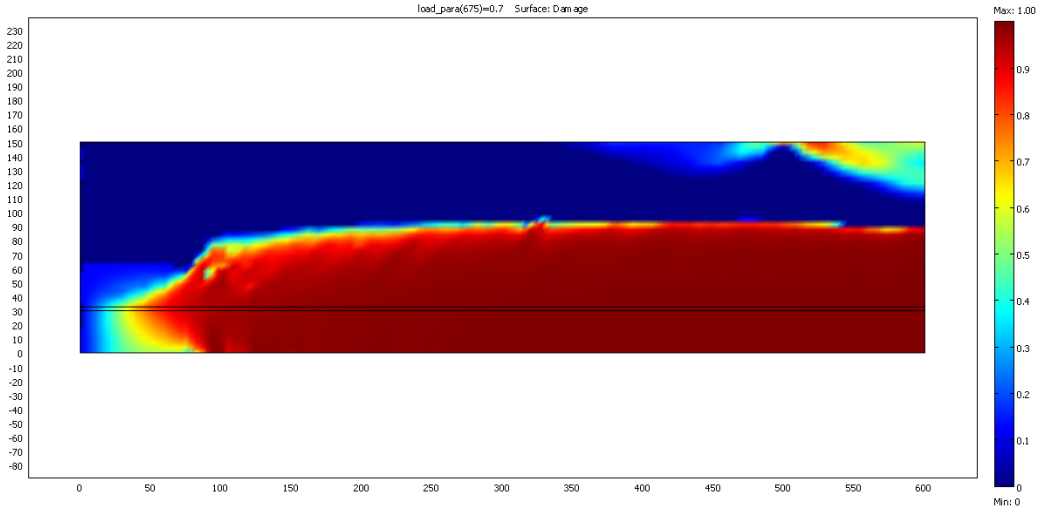


**Figure 21. Scalar Damage $d$ at 90 % Loading Beam B90.**

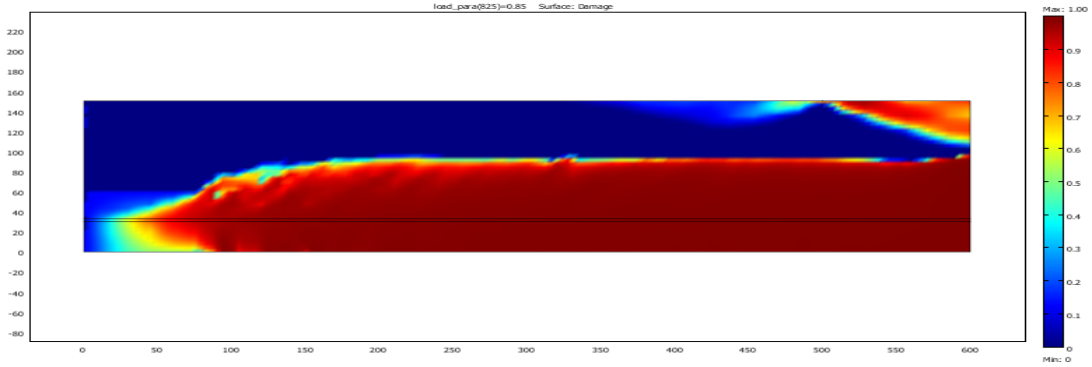


**Figure 22. Scalar Damage $d$ at Failure Loading.**

More details about the development of mechanical damage along the cross section of the RC beam is shown in Fig. 23, where the scalar damage *d* was plotted along the cross section at the constant moment zone. From Fig. 23, it can be noted that at the constant moment zone, the tensile damage is more than 0.90 up to a depth of 80 mm for all damaged RC beams due to higher tensile stress in this region. Besides, the compressive damage was initiated when the RC beams were subjected to 75 % of their ultimate flexural loading and this indicates that the compressive damage propagated at lower rates compared with the tensile damage due to the fact that the concrete sustained more compressive stress than tensile damage.

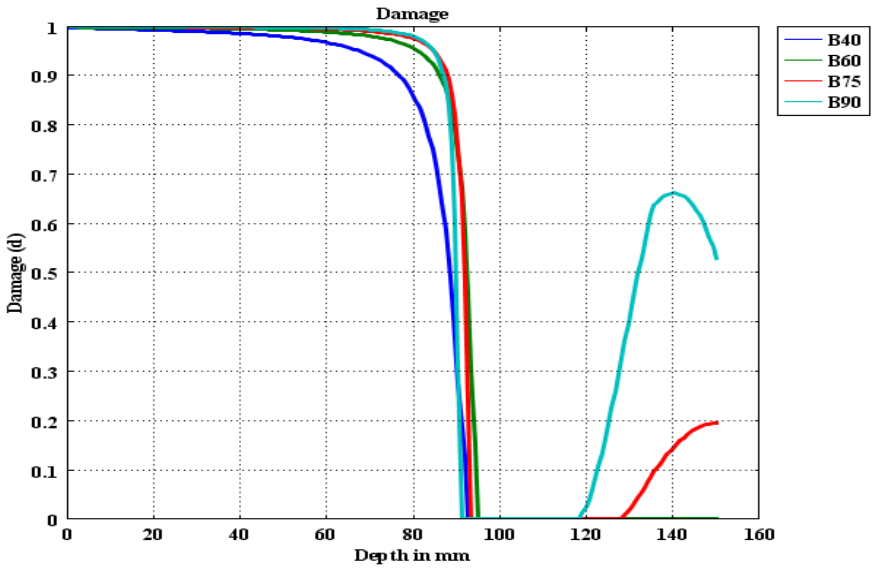


**Figure 23. Damage Distribution across the Beam Section at Mid Span (Constant Moment Zone, $x$ = 550 mm).**

### *3.3.5 Cracks Development in RC Beams*

To verify the COMSOL model with experimental results at crack positions in RC beams with different loading levels, the axial strain ($\varepsilon_x$) was plotted at crack positions in the RC beams as shown in Fig. 24 through 27. It was assumed that the crack would propagate when ($\varepsilon_x$) is more than the crack normal strain ($\varepsilon_{cr}$ = 1.55 × 10$^{-3}$). Fig. 24 shows the normal strain ($\varepsilon_x$) along the position of cracks at distances of 400 and 530 mm from the support in RC beams subjected to 40 % of their ultimate flexural loading. From Fig. 24, it can be noted that the crack depths were found to be about 75 and 85 mm at distances of 400 and 530 mm, respectively, and these results match well with experimental crack maps shown in Fig. 12. The number of cracks and the crack depths increase with the increase of the applied flexural loading. As shown in Fig. 25, the crack depths were increased as the applied flexural loading increased up to 60 % of ultimate loading and were about 82 and 90 mm from crack positions at distance of 360 and 540 mm from the support of the RC beam. One more crack was developed when the RC beams were loaded up to 75 % of their flexural loading as shown in Fig. 26. The crack depths were found to be 50, 85, and 90 mm for cracks at distances of 95, 400 and 520 mm, respectively, from the support of the RC beam. Fig. 27 shows the normal strain ($\varepsilon_x$) at RC beams subjected to 90 % flexural loading and it can be noted that the crack depths were 70, 87 and 90 mm for cracks at distances of 100, 400, and 550 mm, respectively.

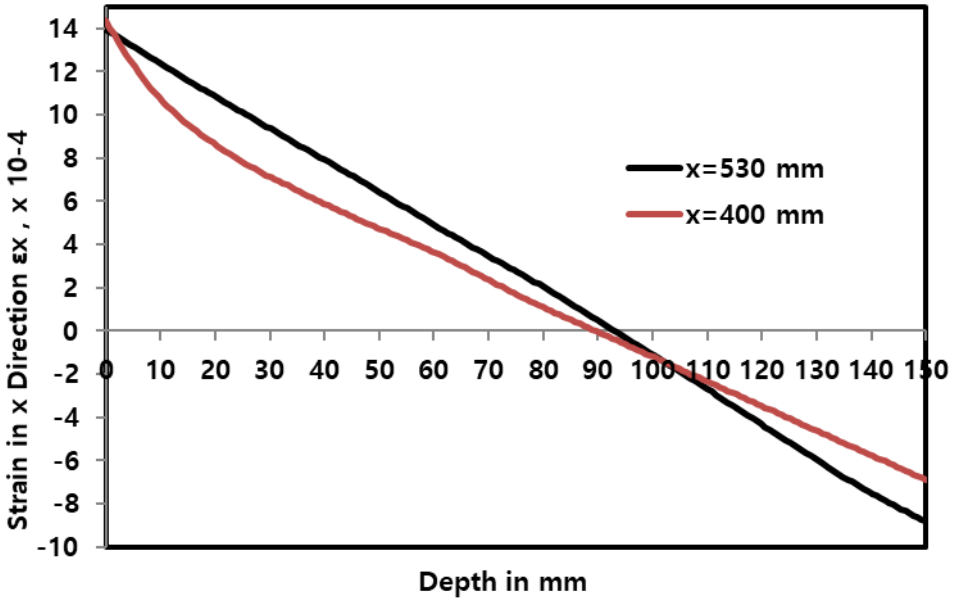


**Figure 24. Axial Strain $\varepsilon_x$ at Cracks in $x$ = 530 mm and $x$ = 400 mm for B40.**

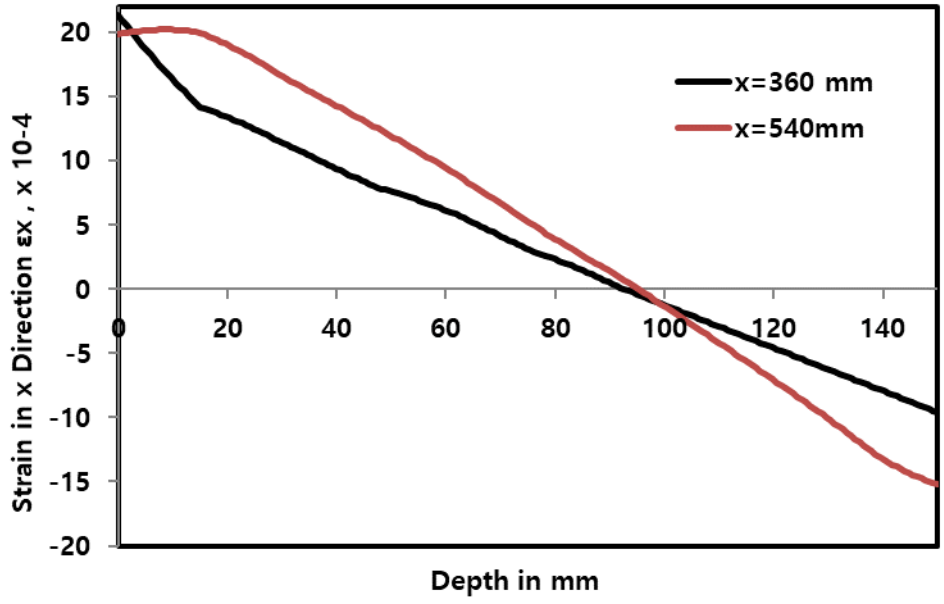


**Figure 25. Axial Strain $\varepsilon_x$ at Cracks in $x$ = 540 mm and $x$ = 360 mm for B60.**

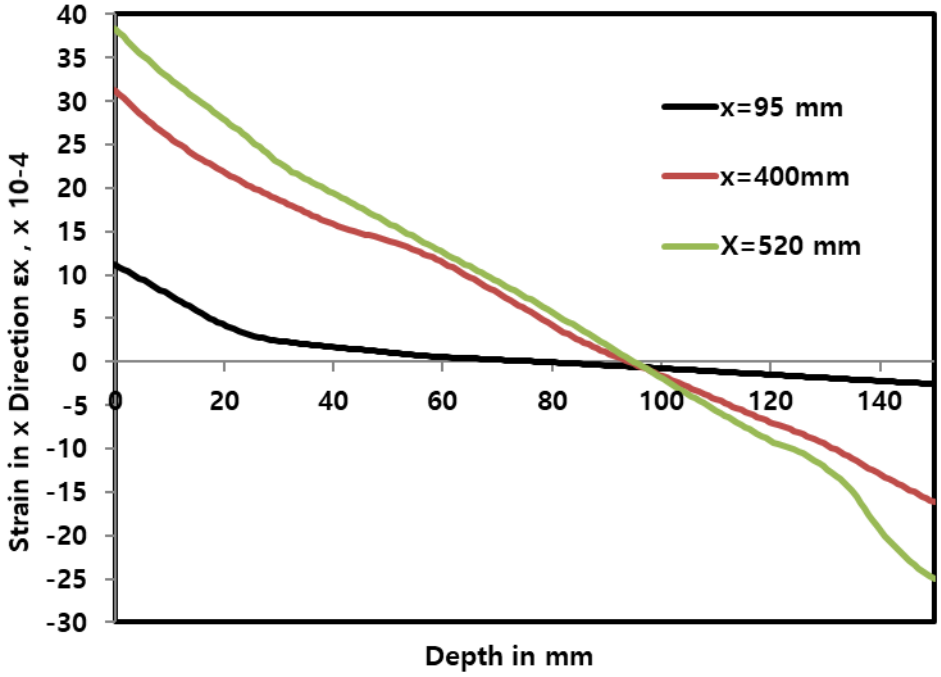


**Figure 26. Axial Strain $\varepsilon_x$ at Cracks in $x$ = 95, 400 and 520 mm for B75.**

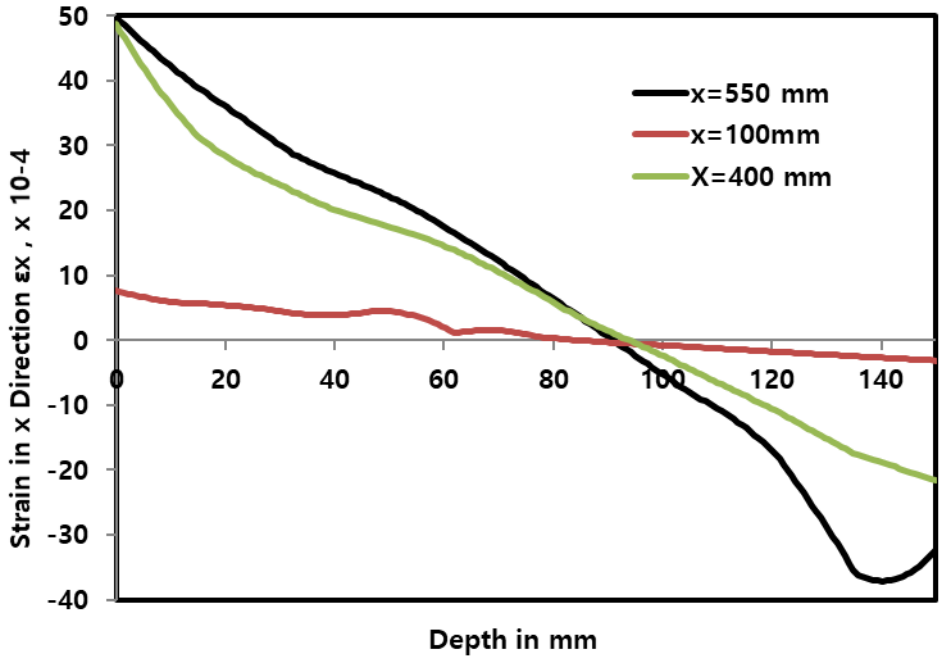


**Figure 27. Axial Strain $\varepsilon_x$ at Cracks in $x$ = 100, 400 and 550 mm for B90.**

## 4. Conclusions

1. An experimental and FE analysis study using a elasto- damage model was conducted to simulate the failure of RC beams subjected to 40 %, 60 %, 75%, and 90 % of ultimate flexural loading.

2. The numerical finite element solution using the COMSOL package was calibrated using load-deflection and reinforcement axial strain experimental results. Besides, empirical formulas for crack depth and spacing were used in this study.

3. The proposed elasto- damage model predicted an ultimate load with 94 kN compared to 95 kN achieved in the experimental flexural tests with 1 % error. The proposed model showed similar ability to predict the axial strain for the reinforcement steel as the maximum strain in tensile reinforcement was found to be 3500 μm at the maximum mid-span deflection of about 7.5 mm these results match well with the experimental results.

4. The accuracy of these results were compared with other constitutive models for concrete such as elasto-plastic damage model reported in literature in which those models were predicted the ultimate loads in RC beams with 4 % estimated error.

5. The numerical results match well with the proposed scalar damage parameters based on an elasto-damage constitutive model. The outcome of this research paper provides engineers a simplified approach for analyzing the behavior of RC beams subjected to flexural loading using elasto- damage model.

## References


1. Kachanov, L. Time of the rupture process under creep conditions. Izvestiia Akademii Nauk SSSR, Otdelenie Teckhnicheskikh Nauk. 1958. 8. Pp. 26–31.
2. Mazars, J., Pijaudier-Cabot, G. Continuum damage theory: Application to concrete. ASCE J Engng Mech. 1989. 115. Pp. 345–365.
3. Taher S., Baluch, M.H., Al-Gadhib, A.H. Towards a canonical elastoplastic damage model. Eng. Fract Mech. 1994. 48 (2). Pp. 151–66.
4. Sun Ming, Xin Dabo, Zou Chaoying. Damage evolution and plasticity development of concrete materials subjected to freeze-thaw during the load process. Mechanics of Materials. 2019. 139. Pp. 103–192.
5. Sarikaya, A. and Erkmen, R.E. A plastic-damage model for concrete under compression. International Journal of Mechanical Sciences. 2019.150. Pp. 584–593.
6. Javanmardi, M.R., and Mahmoud, R. Maheri. Extended finite element method and anisotropic damage plasticity for modelling crack propagation in concrete. Finite Elements in Analysis and Design. 2019. 165. Pp. 1–20.
7. Benin, A.V., Semenov, A.S., Semenov, S.G., Beliaev, M.O., Modestov, V.S. Methods of identification of concrete elastic-plastic-damage models. Magazine of Civil Engineering. 2017. 76(8). Pp. 279–297.
8. Bilal, A., George Z.Voyiadjisb, Taehyo Parka. Damaged plasticity model for concrete using scalar damage variables with a novel stress decomposition. International Journal of Solids and Structures. 2019. https://doi.org/10.1016/j.ijsolstr.2019.11.023
9. Roberto, S., Renato, V., Anna, S., Eugenio,O., Alex, H. A scalar damage model with a shear retention factor for the analysis of reinforced concrete structures: theory and validation. Computers and structures. 2001. 79 (7). Pp. 737–755.
10. Voyiadjis, G.Z., Taqieddin, Z.N., Kattan, P.I. Theoretical formulation of a coupled elastic-plastic anisotropic damage model for concrete using the strain energy equivalence concept. Int.J Damage Mech. 2009. 18 (7). Pp. 603–68.
11. Lubliner, J., Oliver, J., Oller, S., Onate, E. A plastic-damage model for concrete. International Journal of Solids and Structures. 1989. 25 (3). Pp. 299–326.
12. Luccioni, B.M., Rougier, V.C. A plastic damage approach for confined concrete. Computers & Structures. 2005. 83 (27). Pp. 2238–2256.
13. Salari, M.R., Saeb, S., Willam, K.J., Patchet, S.J., Carrasco, R.C. A coupled elastoplastic damage model for geomaterials. Comp. Meth. In Applied Mech. and Eng. 2004. 193 (27). Pp. 2625–2643.
14. Armero, F., Oller, S. A general framework for continuum damage models. I. Infinitesimal plastic damage models in stress space. International Journal of Solids and Structures. 2000. 37 (48-50). Pp. 7409–7436.
15. Labadi, Y., Hannachi, N.E. Numerical simulation of brittle damage in concrete. Strength of Materials. 2005. 37. Pp. 268–281.
16. Tao, X., Phillips, D.V. A simplified isotropic damage model for concrete under bi-axial stress states. Cement and Concrete Composites. 2005. 27 (6). Pp. 716–726.
17. Khan, R.K., Al-Gadhib, A.H., Baluch, M.H. Elasto-damage constitutive model for high strength concrete. Proc. EURO-C Conf. Computational Modeling of Concrete Structures.Austria.1998. Pp. 133–42.
18. Al-Kutti, W.A., Muhammad, K.R., Shazali, M.A., Baluch, M.H. Enhancement in chloride diffusivity due to flexural damage in reinforced concrete beams. Journal of Materials in Civil Engineering. 2014. 26 (4). Pp. 658–667.
19. Willam, K., Rhee, I., Beylkin, G. Multiresolution analysis of elastic degradation in eterogeneous materials. Meccanica. 2001. 36(1). Pp. 131–150.
20. Júnior, F.S., Venturini, W.S. Damage modelling of reinforced concrete beams. Advances in Engineering Software. 2007. 38 (8-9). Pp. 538–546.
21. Khabidolda, O., Bakirov, Zh.B., Nuguzhinov, Zh.S., Vatin, N.I. Determining stress intensity factor in bending reinforced concrete beams. Bulletin of the Karaganda University-Mathematics. – 2019. – Volume 92. – Issue 4. – Pp. 139–147.
22. Popovics S. A numerical approach to the complete stress-strain curve of concrete. Cem Conc Res. 1973. 3. Pp. 583–99.
23. ACI 224 R1.01 Control of Cracking in Concrete Structures, ACI, 2001.
24. COMSOL Multiphysics. User guide (http://www.comsol.com). 2012
25. Abdulsamee, M.H., Yazan B.A., Amin, H.A., George Z.V. The effect of shape memory alloys on the ductility of exterior reinforced concrete beam-column joints using the damage plasticity model. Engineering Structures. 2019. 200. Pp.109676.
26. Elghazy, M., El Refai, A., Usama, E., Antonio, N. Experimental results and modelling of corrosion-damaged concrete beams strengthened with externally-bonded composites. Engineering Structures. 2018. 172. Pp. 172–186.
27. Stéphanie, F., La Borderie, C., Gilles Pijaudier-Cabot. Isotropic and anisotropic descriptions of damage in concrete structures. Mechanics of Cohesive-frictional Materials. 1999. 4(4). Pp. 339–359.


### *Contacts:*


*Walid Al-Kutti, wasalem@iau.edu.sa*
*Tamara Chernykh, chernykhtn@susu.ru*